Interval Demand Response Potential Evaluation and Risk Dispatch to Incorporate Public Buildings into Power System Operation

Yu Yao, Chengjin Ye, Yuming Zhao, and Yi Ding

***Abstract*—Public buildings present substantial demand response (DR) potential, which can participate in the power system operation. However, most public buildings exhibit a high degree of uncertainties due to incomplete information, varying thermal parameters, and stochastic user behaviors, which hinders incorporating the public buildings into power system operation. To address the problem, this paper proposes an interval DR potential evaluation method and a risk dispatch model to integrate public buildings with uncertainties into power system operation. Firstly, the DR evaluation is developed based on the equivalent thermal parameter (ETP) model, actual outdoor temperature data, and air conditioning (AC) consumption data. To quantify the uncertainties of public buildings, the interval evaluation is given employing the linear regression method considering the confidence bound. Utilizing the evaluation results, the risk dispatch model is proposed to allocate public building reserve based on the chance constrained programming (CCP). Finally, the proposed risk dispatch model is reformulated to a mixed-integer second-order cone programming (MISOCP) for its solution. The proposed evaluation method and the risk dispatch model are validated based on the modified IEEE 39-bus system and actual building data obtained from a southern city in China.**

***Index Terms*—Public building, demand response, potential evaluation, risk dispatch, chance constrained programming, power system operation.**

I. Introduction

THE penetration of renewable energy is burgeoning to deal with the electricity consumption increase and carbon emission reduction [1]. The high share of renewable energy brings more uncertainties and replaces the traditional flexibility resources such as thermal generators, which requires more flexible resources to ensure the stable operation of the power system [2]. With the advancement of information and communication technology, demand response (DR) has been effectively employed in practical engineering to enhance the regulation capabilities of power systems [3].

Public buildings present significant potential for participating in DR. Firstly, public buildings contribute about 39% proportion of global energy consumption [4]. Secondly, public buildings, which are frequently managed centrally by property management companies, are more susceptible to uniform scheduling and management. Furthermore, air conditioning (AC) systems, which consume 50% of the electricity of a public building [5], exhibit thermal inertia, allowing for brief shut-downs or power reductions with a small impact on consumers.

Compared with traditional thermal generators, most public buildings have a high degree of uncertainties due to the lack of complete information, constant thermal parameters, and deterministic user behaviors, which hinders integrating the high-potential public buildings into power system operation. Furthermore, the majority of public buildings have no advanced building automation systems (BASs) or communication networks, which results in the lack of key operation data [6]. Some varying envelop parameters for DR potential evaluation need to be measured through experiments [7], which is infeasible for large-scale public buildings. The behavior of building occupants and their comfort requirements are heterogeneous and stochastic [8]. Therefore, most public buildings in actual engineering will produce a significant amount of uncertainties in power system dispatch.

The primary research for incorporating public buildings into power system operation is the DR potential evaluation and quantification. An accurate and practical potential evaluation method is important for load aggregators (LAs) or independent system operators (ISOs) to schedule public buildings. Numerous researches have been conducted on potential evaluation for public buildings. On the one hand, detailed models of public buildings and AC systems are constructed to conduct the DR potential evaluation, which needs multiple parameters and complete information [9]. Reference [10] proposes a coupled thermal inertia model considering public buildings and AC systems to quantify the DR contributions of the public buildings. The model requires detailed room parameters such as material, density, and heat conduction coefficient. For most public buildings, it is difficult to obtain

Manuscript received: August 19, 2024; revised: November 6, 2024; accepted: December 24, 2024. Date of CrossCheck: December 24, 2024. Date of online publication: January 28, 2025.

This work was supported by the National Science Fund for Distinguished Young Scholars (No. 52125702) and the Key Science and Technology Project of China Southern Power Grid Corporation (No. 090000KK52220020).

Y. Yao, C. Ye (corresponding author), and Y. Ding are with the College of Electrical Engineering, Zhejiang University, Hangzhou, China (e-mail: eeyuyao@zju.edu.cn; yechenjing@zju.edu.cn; yiding@zju.edu.cn).

Y. Zhao is with Shenzhen Power Supply Bureau Co., Ltd., Shenzhen, China (e-mail: zhaoym97@sina.com).

DOI: 10.35833/MPCE.2024.000919

these parameters. In [11], the detailed public building parameters are extracted by an active experiment. Moreover, the DR potential of public buildings is studied. Also, the detailed parameters of the test room are necessary to construct the potential evaluation model. Reference [12] conducts DR potential evaluation to reduce peak demand for a medium-sized public building considering integrated dynamic window and heating, ventilation, and air conditioning (HVAC) systems. Multiple input parameters are required to construct the model predictive control algorithm, which is more suitable for simulation. In summary, most methods are only applicable to public buildings with complete information. Although these methods can achieve more accurate evaluations in simulations, they are challenging to implement effectively in practice. On the other hand, data-driven methods are applied to evaluate the DR potential, which needs a huge amount of data [13]. Reference [13] proposes a public building potential evaluation method that combines federated learning and transfer learning methods. In [14], a data-driven method is proposed to quantify the adjustable capacity of individual flexible loads. Reference [15] proposes a data-driven method to rapidly quantify the DR potential of HVAC.

The above methods of evaluating DR potential require extensive building parameters and high-quality operational data. However, it is challenging to obtain these parameters and data in practice, which induces uncertainties in the DR potential evaluation of public buildings. In addition, human behaviors and some key parameters such as building envelop and AC operation data are varying, also bringing uncertainties to public buildings. These uncertainties should be considered during the evaluation process, which have not been addressed in existing research. To fill the research gap, the interval prediction method can be employed as an appreciated tool to model these uncertainties, which has been applied in photovoltaic power prediction [16], [17] and electricity price prediction [18]. In [16], an interval prediction method combining the lower and upper bound estimations is proposed to characterize the uncertainty of solar power prediction. Reference [17] proposes a method combining granule-based clustering and direct optimization programming to improve the performance of very short-term regional photovoltaic output prediction [17]. Reference [18] forecasts the electricity price with the optimal prediction interval method. To the author's best knowledge, the interval prediction method in existing research has not been utilized to evaluate the DR potential of public buildings, especially public buildings with uncertainties concerned in this paper.

Most of the existing research works concentrate on the energy management of public buildings and coordination with power systems, which realizes the reduction of energy consumption. In [19], a hierarchical optimal method is proposed to schedule flexibility offered as transactive energy by thermostatically controlled loads in public buildings. Reference [20] proposes a convex formulation for commercial building operation and optimization. Moreover, a privacy-preserving algorithm is utilized to realize the coordination of multiple public buildings connected to power networks. In [21], an optimal algorithm is proposed to conduct the charging and discharging dispatch of a thermal energy storage system and a battery energy storage system, which realizes the cost reduction of building operations. Reference [22] presents an optimal strategy based on online learning of interconnected neural networks to optimize the operation of HVAC system in a commercial building. Nonetheless, these research works focus on the economic operation of public buildings and power systems, failing to consider the impact of public building uncertainties on the power system. Although some researchers have conducted some risk dispatch schemes, they aim to solve the uncertainties caused by the renewable energy and electricity load [23]. Consequently, the uncertain public buildings cannot effectively participate in and even adversely affect the system operation.

In summary, there are two main gaps in the research on integrating public buildings into power system dispatch: DR potential evaluation of public buildings considering uncertainties; and coordinated dispatch method of uncertain public buildings and traditional power system resources. To cope with the above research gaps, this paper proposes an interval DR potential evaluation method (hereafter named the proposed evaluation method) and a risk dispatch model to incorporate public buildings with uncertainties into power system operation. The contributions are summarized as follows.

1) Based on the equivalent thermal parameter (ETP) model, the proposed evaluation method for public buildings is developed. Considering the uncertainties of public buildings, the interval DR potential evaluation model is constructed utilizing linear regression considering confidence bounds. The proposed evaluation method delivers credible evaluation results of public buildings with uncertainties.

2) Based on the evaluation results, a risk dispatch model is proposed to allocate the thermal generator reserve and uncertain public building reserve employing the chance constrained programming (CCP). The proposed risk dispatch model can conduct dispatch schemes for different requirements of confidence level, which realizes a balance between risk and cost. The proposed risk dispatch model is reformulated to a mixed-integer second-order cone programming (MISOCP) by the mathematical deduction, which can be effectively solved.

The remainder of this paper is organized as follows. Section II introduces the framework of the proposed evaluation method and risk dispatch model for public buildings with uncertainties. The proposed evaluation method is presented in Section III. Section IV introduces the proposed risk dispatch model. Results and discussion are shown in Section V. The conclusions are given in Section VI.

II. Framework of Proposed Evaluation Method and Risk Dispatch Model for Public Buildings with Uncertainties

Generally, DR potential evaluation and risk dispatch of public buildings in existing research require complete information such as outdoor temperature, AC power, AC operation data, envelope parameter, indoor environment parameter, and indoor heat production data, as shown in Fig. 1. Outdoor temperature is a critical factor affecting the AC power. AC power is the most important data for evaluating the adjustable potential. AC operation data such as energy efficiency ratio, real-time cooling capacity, and water supply temperature are the significant data supporting the potential evaluation of AC. The envelope parameters including thickness, material, and heat transfer coefficient of the wall are crucial when modeling the heat exchange of a public building. Indoor environment parameters such as indoor temperature and humidity can reflect the cooling performance of the AC system. Indoor heat sources including human and appliance are important factors affecting the cooling load of AC.

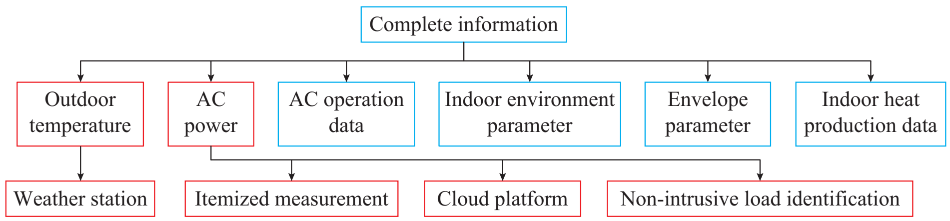

Fig. 1. Complete information of public buildings.

For most existing public buildings in practice, the information available for potential evaluation and risk dispatch is limited. Generally, outdoor temperature and AC power can be easily obtained. Outdoor temperature can be obtained from the weather station near the target public building. AC power can be directly measured in public buildings with submetering. For smart ACs, AC power data are uploaded to a cloud platform. For other public buildings, non-invasive load identification methods can be utilized to indirectly extract AC power data. However, it is challenging to collect AC operation data, envelope parameter, indoor environment parameters, and indoor heat production data. Obtaining these complete parameters requires the original construction drawings of public buildings, modifications to the AC system, and the installation of additional sensors, which is infeasible for large-scale existing public buildings. In addition, there are some fluctuations in human behaviors and parameters such as building envelope, indoor heat production, and AC operation state. Therefore, the public buildings exhibit some uncertainties due to the lack of information and the fluctuations of data. Compared with traditional thermal generators, it is difficult to integrate these public buildings into power system operation.

To address the problem of incorporating the public buildings into power system operation, the proposed evaluation method and risk dispatch model are presented, whose framework is shown in Fig. 2. Firstly, LAs evaluate the DR potential of aggregated public buildings, containing the utility, mall, commercial office, hotel, etc. The proposed evaluation method can mitigate the uncertainty arising from limited information, providing credible DR potential evaluation results. Then, LAs upload the adjustable potential and uncertainty coefficient of heterogenous public buildings to ISO. Furthermore, the ISO conducts the reserve allocation based on the interval DR potential. Utilizing the proposed risk dispatch model, a balance between dispatch cost and risk is achieved. Consequently, the reserve allocation plan is downloaded to the LAs.

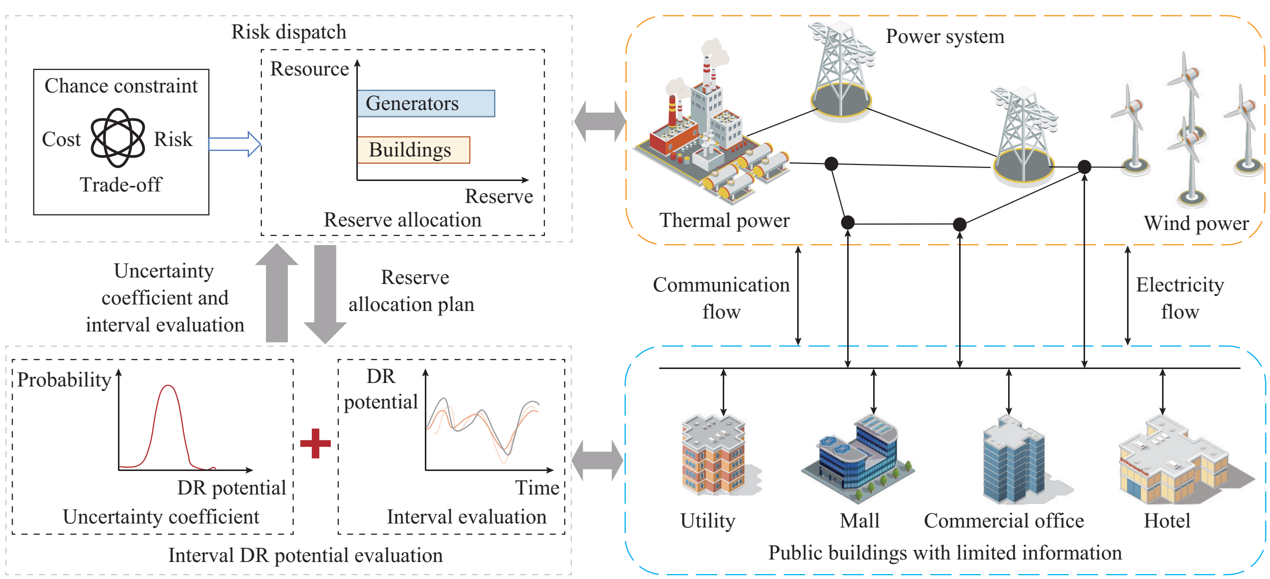

Fig. 2. Framework of proposed evaluation method and risk dispatch model for uncertain public buildings.

III. Proposed Evaluation Method

The thermal dynamic process of the room is illustrated in Fig. 3. Solar radiation, outdoor heat transfer, and heat generation of human and appliance are the three main heat sources. The AC produces the cooling air. The indoor air changes due to the cooling and heating sources, which are described by the first-order ETP model [24] shown in Fig. 3.

$$C\frac{\mathrm{d}T_{in}}{\mathrm{d}t}=\frac{T_{out}-T_{in}}{R}-C_{OP}P_{AC}+Q_s+Q_l \tag{1}$$

where C and R are the equivalent thermal capacitance and resistance, respectively; T_{out} and T_{in} are the outdoor and indoor temperatures, respectively; Q_s and Q_l are the solar radiation and heat generation of human and appliance, respectively; and P_{AC} and C_{OP} are the AC power and energy efficiency, respectively.

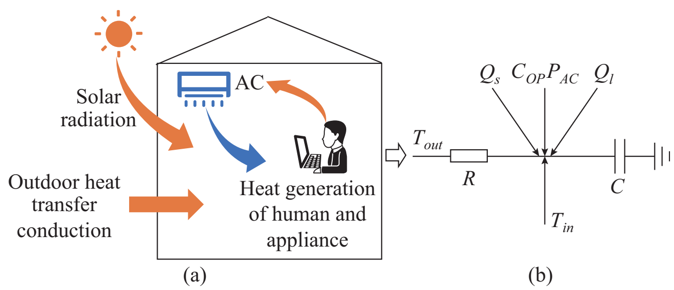

Fig. 3. Thermal dynamic process and the first-order ETP model. (a) Thermal dynamic process. (b) The first-order ETP model.

When the indoor temperature enters a steady period, AC power also maintains a relatively constant value:

$$P_{AC}=\frac{T_{out}-T_{in}}{C_{OP}R}+\frac{Q_s+Q_l}{C_{OP}} \tag{2}$$

Generally, the indoor temperature can be maintained to temperature setting T_{set} by ACs:

$$P_{AC}=\frac{T_{out}-T_{set}}{C_{OP}R}+\frac{Q_s+Q_l}{C_{OP}} \tag{3}$$

C_{OP} will constantly change during real-time operation. R will vary with the opening and closing of the room windows. Q_s and Q_l will also change at different time. Therefore, the variation of these parameters creates difficulties in the DR potential evaluation of public buildings. In the evaluation, the uncertainties of these parameters should be considered. Equation (3) illustrates that P_{AC} is linearly correlated with the difference between T_{out} and T_{set}. Furthermore, (3) can be simplified to (4)-(6).

$$P_{AC}=\alpha(T_{out}-T_{set})+\beta \tag{4}$$

$$\alpha=\frac{1}{C_{OP}R} \tag{5}$$

$$\beta=\frac{Q_s+Q_l}{C_{OP}} \tag{6}$$

where α and β are the linear term and constant term, respectively. Generally, T_{set} remains relatively constant, especially for large centralized AC systems. Therefore, (4)-(6) can be deducted as (7) and (8).

$$P_{AC}=\alpha T_{out}+\beta \tag{7}$$

$$\beta=\frac{Q_s+Q_l}{C_{OP}}-\frac{1}{C_{OP}R}T_{set} \tag{8}$$

That is to say, T_{set} only affects β. The slope α can be fitted utilizing T_{out} and P_{AC} data.

Power reduction can be conducted by raising the temperature setting of AC, so that the AC participates in DR. Moreover, the DR potential of AC power can be expressed as:

$$\Delta P_{AC}=\alpha\Delta T_{set} \tag{9}$$

where ΔP_{AC} is the DR potential; and ΔT_{set} is the change of temperature setting.

Linear regression is carried out based on historical AC power and outdoor temperature data. The residual sum of the square between the original and predicted data [25] is constructed as:

$$Q=\sum_{i=1}^{n}(P_{ACi}-\hat{P}_{ACi})^2=\sum_{i=1}^{n}[P_{ACi}-(\hat{\alpha}T_{outi}+\hat{\beta})]^2 \tag{10}$$

where Q is the total squared value; and $\hat{P}_{ACi}$ is the predicted AC power of the i^{th} AC; and $\hat{\alpha}$ and $\hat{\beta}$ are the predicted coefficients of α and β, respectively.

The extreme values of the target can be taken when the partial derivatives of the two parameters are zero [24].

$$\frac{\partial Q}{\partial \alpha}=-2\sum_{i=1}^{n}[P_{ACi}-(\hat{\alpha}T_{outi}+\hat{\beta})]T_{outi}=0 \tag{11}$$

$$\frac{\partial Q}{\partial \beta}=-2\sum_{i=1}^{n}[P_{ACi}-(\hat{\alpha}T_{outi}+\hat{\beta})]=0 \tag{12}$$

However, α and β include uncertain parameters such as R, C_{OP}, Q_s, and Q_l. Therefore, the two parameters should be presented in an uncertain form. As shown in Fig. 4, we present the confidence bounds on coefficients to describe the uncertainties of two parameters [24].

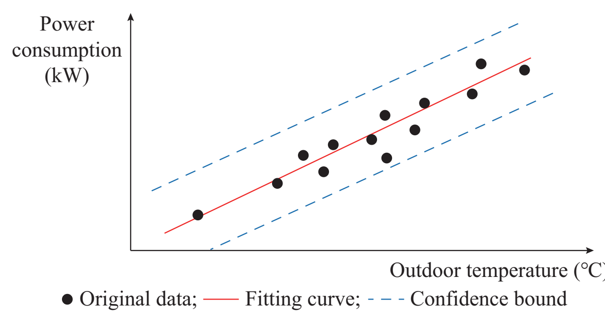

Fig. 4. Linear regression considering confidence bounds.

$$\alpha_{interval}=\hat{\alpha}\pm t_{C/2,n-p}\hat{\sigma}_{\alpha} \tag{13}$$

$$\beta_{interval}=\hat{\beta}\pm t_{C/2,n-p}\hat{\sigma}_{\beta} \tag{14}$$

where $\alpha_{interval}$ and $\beta_{interval}$ are the confidence bounds of α and β, respectively; $t_{C/2,n-2}$ is the t cumulative distribution function of the student; and $\hat{\sigma}_{\alpha}$ and $\hat{\sigma}_{\beta}$ are the standard deviations of α and β, respectively.

Based on the confidence bounds of coefficients, the interval DR potential $\Delta P_{AC,CL}$ at a certain confidence level CL can be expressed as:

$$\Delta P_{AC,CL}=\alpha_{interval,CL}\Delta T_{set} \tag{15}$$

where $\alpha_{interval,CL}$ is the interval value of α at a certain confidence level.

The interval DR potential can be calculated by (15). However, the minimal DR potential of AC at certain confidence level is more important in actual DR. Therefore, the downward bound is taken as the parameter to calculate the DR potential.

$$\Delta P_{AC,CL} = \underline{\alpha}_{interval,CL} \Delta T_{set} \tag{16}$$

where $\underline{\alpha}_{interval,CL}$ is the downward bound of α at a confidence level. A series of evaluation results are given at different confidence levels, which provide more information for LAs or ISOs.

The fitted coefficient $\alpha_{interval}$ meets the student distribution [26]. When the number of samples exceeds 30, the *t*-distribution gradually approaches a normal distribution [27]. Therefore, the fitted coefficient $\alpha_{interval}$ meets the distribution $N(\hat{\alpha}, \sigma_\alpha^2)$. Furthermore, the uncertainty coefficient ξ can be deducted as:

$$\xi = \frac{\Delta P_{AC}^{uncertain}}{\Delta P_{AC}^{certain}} = \frac{\alpha_{interval} \Delta T_{set}}{\alpha \Delta T_{set}} = \frac{\alpha_{interval}}{\alpha} \tag{17}$$

where $\Delta P_{AC}^{uncertain}$ is the uncertain DR potential; and $\Delta P_{AC}^{certain}$ is the certain DR potential.

Therefore, the uncertainty coefficient follows the distribution $N(1, \sigma_\alpha^2/\alpha^2)$.

In fact, there are many sources of uncertainties in public buildings. As shown in Fig. 5, the uncertainties affecting the potential evaluation of public building include incomplete information, parameter variation, control accuracy, human activity, and weather forecasting error. Incomplete information means a lack of necessary data required for public building potential evaluation, such as AC operation data, indoor environment parameter, envelope parameter, and indoor heat production. In addition, some parameters vary in real-time, which introduces uncertainties into the DR potential evaluation of public buildings. For example, the energy efficiency ratio of AC can vary with changes in load rates. The equivalent thermal resistance of a public building can significantly change with the opening and closing of doors and windows. Solar radiation and heat generation of human and appliance also vary in real time.

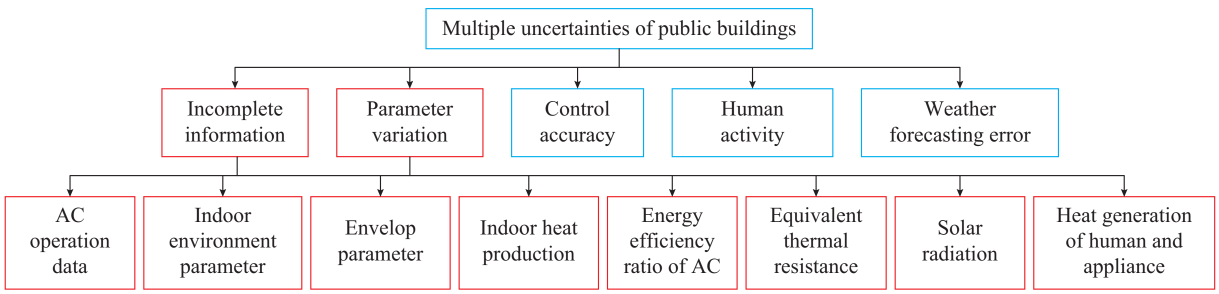

Fig. 5. Multiple uncertainties of public buildings.

The uncertainties addressed in this paper are the red boxes in Fig. 5, specifically the uncertainties arising from the incomplete information and parameter variations. On the one hand, incomplete information makes it difficult to construct detailed models for public buildings and AC systems. As a result, previously used detailed simulation software like Energy Plus lacks the relevant parameters, making it challenging to create refined models for the potential evaluation of public buildings. However, the proposed evaluation method and risk dispatch model only require historical AC power and outdoor temperature data. With simple linear regression, an AC system model and DR potential evaluation model can be constructed, effectively addressing the uncertainties caused by insufficient information. On the other hand, parameter variations also introduce uncertainties to potential evaluation. As shown in (3), the parameters C_{OP}, R, Q_s, and Q_l have effects on the fitting results. C_{OP}, R, Q_s, and Q_l will vary in the real-time operation. C_{OP} changes with variations in AC load rate and indoor and outdoor temperatures. R changes with the opening and closing of doors and windows in the public building. Solar radiation and heat generation of human and appliance also vary in real time. Variations in these parameters will introduce uncertainties into the results of the potential evaluation. Although many uncertain parameters are changing in real time, the proposed evaluation method can overcome these uncertainties and provide a potential evaluation result at a certain confidence level.

IV. Proposed Risk Dispatch Model

Considering the uncertainties of parameters and evaluation results, the risk dispatch model is proposed to develop a reserve dispatch plan for large-scale public buildings. The CCP is utilized in the proposed risk dispatch model to make a trade-off between risk and cost. The time scale of the proposed evaluation method and risk dispatch model are both day-ahead. The proposed evaluation method provides potential evaluation results on a day-ahead time scale due to the limitation of insufficient data collection. Real-time and detailed evaluation of DR potential needs more data. For the dispatch, besides arranging the thermal generator reserve and public building reserve, the on-off plans of the thermal generators also need to be scheduled. In actual operation, the on-off plans of thermal generator are arranged on a day-ahead basis. As large-scale public buildings gradually participate in DR, more public buildings will be directly connected to the ISO. There is a need to schedule public buildings with uncertainties and simultaneously arrange thermal generator reserves, public building reserves, and on-off plans of thermal generators on a day-ahead basis.

A. Standard Form of CCP

CCP is a method that integrates uncertainty into optimization problems. By incorporating probability into the constraints, CCP ensures that these constraints are met at a specified confidence level *CL*, thereby addressing the impact of random variables. A standard form of CCP is [28]:

$$\begin{cases} f(x_1, x_2, ..., x_n) \\ \text{s.t. } \Pr\{a_1 x_1 + a_2 x_2 + ... + a_n x_n - b \le 0\} \ge CL \end{cases} \tag{18}$$

where $f(\cdot)$ is the objective function; $x_1, x_2, ..., x_n$ are the decision variables; $a_1, a_2, ..., a_n$ and b are the uncertainty coefficients, which met the individual Gaussian distribution; and $\Pr\{\}$ is the chance constraint. Utilizing the mathematical method [29], the chance constraint in (18) can be conducted as:

$$\sum_{i=1}^{n}[E(a_i)x_i - E(b_i) + \varphi^{-1}(CL)]\sqrt{\sum_{i=1}^{n} V(a_i)x_i^2 + V(b_i)} \le 0 \tag{19}$$

where $E(\cdot)$ and $V(\cdot)$ are the expectation and variance of the uncertainty coefficient, respectively; b_i is the uncertainty coefficient; and $\varphi^{-1}(CL)$ is the inverse function of the normal distribution $N(0, 1)$.

B. Objective Function

The objective function is the minimal total cost of fuel, reserve, and wind power prediction deviation:

$$\begin{cases} \min(F_{Fuel} + F_{Reserve} + F_{Wind}) \\ F_{Fuel} = \sum_{t=1}^{N_T}\sum_{g=1}^{N_G}[C_g^{SU} Y_{g,t}^G (1 - Y_{g,t-1}^G) + (aP_{g,t}^2 + bP_{g,t} + c)] \\ F_{Reserve} = \sum_{t=1}^{N_T}\sum_{g=1}^{N_G} C_g^R R_{g,t}^G + \sum_{i=1}^{N_{building}} C_i^{building} R_{i,t}^{building} \\ F_{Wind} = \sum_{t=1}^{N_T}\sum_{g=1}^{N_W} C^w (\gamma_{w,t} P_w^{\max} - P_{w,t}) \end{cases} \tag{20}$$

where t denotes the time; F_{Fuel}, $F_{Reserve}$, and F_{Wind} are the fuel, reserve, and wind power prediction deviation costs, respectively; N_T, N_G, $N_{building}$, and N_W are the numbers of time units, thermal generators, public buildings, and wind power generators, respectively; C_g^{SU} and C_g^R are the starting up and reserve cost coefficients of the thermal generator, respectively; a, b, and c are the fuel cost coefficients of thermal generators; $C_i^{building}$ and C^w are the reserve cost coefficient and wind power prediction deviation cost coefficient of the public building, respectively; $Y_{g,t}^G$, $P_{g,t}$, and $R_{g,t}^G$ are the on/off status variable, power output, and reserve of the thermal generator, respectively; $R_{i,t}^{building}$ is the public building reserve; and $\gamma_{w,t}$, $P_w^{\max}$, and $P_{w,t}$ are the output ratio, maximum output, and the real output of the wind power generator, respectively.

C. Constraints

1) Power Balance Constraint

Constraint (21) ensures the power balance of the power system in each time:

$$\sum_{g=1}^{N_G} P_{g,t} + \sum_{i=1}^{N_W} P_{w,t} = P_t^{Load} \quad \forall t \tag{21}$$

where P_t^{Load} is the power load of the whole power system.

2) Thermal Generator Constraints

Constraint (22) limits the power generation of all thermal generators to their respective capacities. The on/off status of these thermal generators is governed by constraints (23)-(25). The minimum online time and offline time are restricted by constraints (26) and (27). Constraint (28) imposes limits on the ramping rate of each thermal generator.

$$Y_{g,t}\underline{P}_g \le P_{g,t} \le Y_{g,t}\bar{P}_g \quad \forall g, \forall t \tag{22}$$

$$Y_{g,t} - Y_{g,t-1} = Y_{g,t}^{on} - Y_{g,t}^{off} \quad \forall g, \forall t \tag{23}$$

$$Y_{g,t}, Y_{g,t-1}^{on}, Y_{g,t-1}^{off} \in \{0, 1\} \quad \forall g, \forall t \tag{24}$$

$$Y_{g,t-1}^{on} + Y_{g,t-1}^{off} \le 1 \quad \forall g, \forall t \tag{25}$$

$$\sum_{\tau=t-T_g^{on}-1}^{t-1} Y_{g,\tau} \ge Y_{g,t}^{off} T_g^{on} \quad \forall g, \forall t \tag{26}$$

$$\sum_{\tau=t-T_g^{off}-1}^{t-1} (1 - Y_{g,\tau}) \ge Y_{g,t}^{on} T_g^{off} \quad \forall g, \forall t \tag{27}$$

$$-RR_g^D \cdot \Delta T \le P_{g,t} - P_{g,t-1} \le RR_g^U \cdot \Delta T \quad \forall g, \forall t \tag{28}$$

where $\bar{P}_g$ and $\underline{P}_g$ are the upper and lower limits of power output of thermal generator g, respectively; $Y_{g,t}^{on}$ and $Y_{g,t}^{off}$ are the on status and off status of thermal generator g, which are binary indicators, respectively; T_g^{off} and T_g^{on} are the minimum offline time and online time of thermal generator g, respectively; and RR_g^D and RR_g^U are the rates of ramp-down and ramp-up of thermal generator g, respectively.

3) Power Flow Constraints

DC power flow of each transmission line can be expressed as (29). Constraint (30) limits the DC power flow of each branch to its capacity.

$$F_{l,t}^L = B_l^L(\theta_{l(+),t} - \theta_{l(-),t}) \quad \forall l, \forall t \tag{29}$$

$$-F_l^{L,\max} \le F_{l,t}^L \le F_l^{L,\max} \tag{30}$$

where $F_{l,t}^L$ is the power flow of transmission line l; $\theta_{l(+),t}$ and $\theta_{l(-),t}$ are the voltage phase angles of the sending end and receiving end, respectively; and B_l^L and $F_l^{L,\max}$ are the susceptance and capacity of transmission line l, respectively.

4) Probability Reserve Constraints

Constraints (31) and (32) limit the maximum capacity of the thermal generator and pubic building reserve. Constraint (33) is the chance constraint, representing the probability that the allocated reserve needs to be greater than the confidence level.

$$0 \le R_{g,t} + P_{g,t} \le \bar{P}_g \quad \forall t \tag{31}$$

$$0 \le R_{i,t}^{building} \le \Delta P_{AC,CL} \quad \forall t \tag{32}$$

$$\Pr\left\{\sum_{g=1}^{N_G} R_{g,t} + \sum_{i=1}^{N_{building}} \xi_i^{building} R_{i,t}^{building} \ge R_{require}\right\} \ge CL \quad \forall t \tag{33}$$

where $R_{require}$ is the reserve required by the power system; and $\xi_i^{building}$ is the uncertainty coefficient. The chance constraint can be transformed to certain constraint utilizing the mathematical method or sample average approximation (SAA) [30]. In the chance constraint (33), the uncertainty coefficient $\xi_i^{building}$ follows a normal distribution, so the mathematical derivation can be utilized to handle the chance constraint. The mathematical derivation method performs better than SAA in terms of computation time, accuracy, and stability. The chance constraint (33) can be further conducted as (34) utilizing (19).

$$\sum_{g=1}^{N_G} R_{g,t} + \sum_{i=1}^{N_{building}} E(\xi_i^{building}) R_{i,t}^{building} - \varphi^{-1}(CL)\sqrt{\sum_{b=1}^{N_{building}} V(\xi_i^{building})(R_{i,t}^{building})^2} \ge R_{require} \quad (34)$$

$\xi_i^{building}$ is uploaded by LAs, which is quantified by (17). Constraint (34) contains second-order cone term and (22)-(28) include binary variables. Therefore, the risk dispatch model is converted to an MISOCP model, which can be efficiently solved utilizing commercial solvers such as GUROBI [31].

V. Results and Discussion

A. Data Sources

The ground truth data come from four public buildings in a city of southern China, which is employed to validate the effectiveness of the proposed evaluation method. Buildings 1 and 2 are cooled by variable refrigerant volume (VRV) systems. Buildings 3 and 4 are equipped with center air conditioning (CAC) systems. The AC power is collected from the building automation control system. The outdoor temperature is measured by the building automation control system or weather station. The data from building 1 pertain to July 2023, with a time scale of minute. For building 2, the data span from May 27, 2024 to June 8, 2024 with a time scale of 30 s. In buildings 3 and 4, the data span from July 1, 2023 to August 31, 2023 with a time scale of min. The outliers of raw data are cleaned using the interquartile range method [32]. In addition, raw data are removed when the AC is off.

The proposed risk dispatch model is validated based on a modified IEEE 39-bus system [33], as shown in Fig. 6.

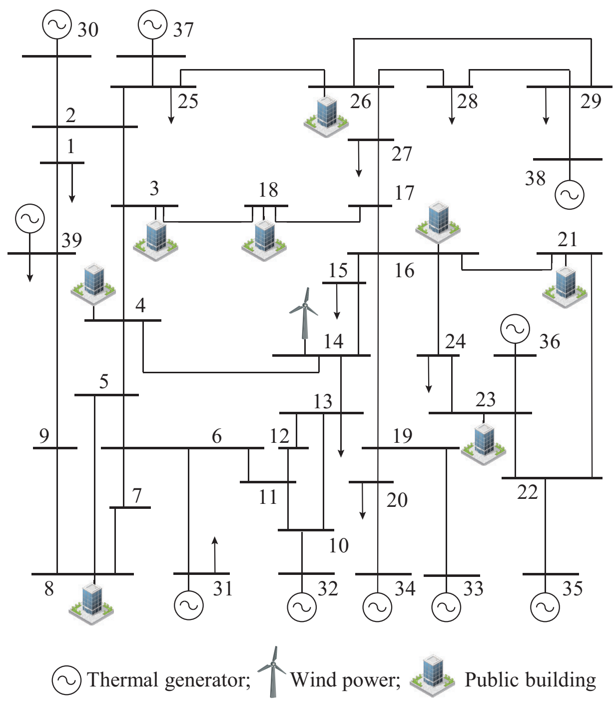

Fig. 6. Modified IEEE 39-bus system.

Table I shows the parameters of ten candidate thermal generators, where $P_g^{\max}$ is the maximum output of thermal generator g. The reserve and start-up cost coefficients are equivalent to c. Bus 14 is connected to a wind power generator. The four public buildings represent four typical building clusters, which are connected with buses 3, 4, 8, and 16. The other four public building clusters are set to be the same as the first four public building clusters, which are connected with buses 18, 21, 23, and 26. The dispatch cost is higher than that of thermal generators, because the load-side flexible resources are more expensive. In Guangdong province, China, the reserve cost for thermal generators is 0.3 ¥/kWh [34]. The reserve cost for demand-side resources reaches up to 3.5 ¥/kWh [35]. Therefore, the cost of demand-side resources can be up to 11 times that of thermal generators. Based on this, the cost coefficient ranges from 0 to 11 times that of thermal generators. Thus, the cost coefficient of the public building is set to be 5 times that of thermal generators 30-37. The total load, wind power output, and AC power of four public buildings are shown in Fig. 7. All simulations were performed on a computer equipped with a 13th Gen Intel(R) Core(TM) i5-13600KF 3.50 GHz CPU and 32.0 GB of RAM. The model used in this study was programmed using MATLAB 2022b YALMIP, and GUROBI 10.0.

TABLE I
Parameters of Ten Candidate Thermal Generators

Generator	$P_g^{\max}$ (MW)	b (\$/MW)	c (\$)	C_g^R (\$)	C_g^{SU} (\$)
30	1040	3.0	700	700	700
31	646	6.5	500	500	500
32	725	5.0	600	600	600
33	652	4.5	600	600	600
34	508	7.0	480	480	480
35	687	6.0	700	500	500
36	580	12.5	500	400	400
37	564	12.0	600	400	400
38	865	5.0	600	600	600
39	1100	2.5	480	800	800

B. Fitting Results Considering Confidence Level

Figure 8 shows the fitting results of the four public buildings at a 95% confidence level. The proposed evaluation method provides good envelopes for most of the points. In contrast, the deterministic evaluation method only provides a fitting curve. The proposed evaluation method considers all possible points, providing more credible results.

Table II presents the fitting parameters for four public buildings at a 95% confidence level, including α, lower bound $\underline{\alpha}$, and uncertainty coefficient σ_α. Taking building 1 as an example, the lower bound at the 95% confidence level differs by 9.46% from the deterministic predicted α. This indicates that even at the 95% confidence level, there is still a significant difference from the deterministic prediction result. Therefore, the proposed evaluation method is necessary.

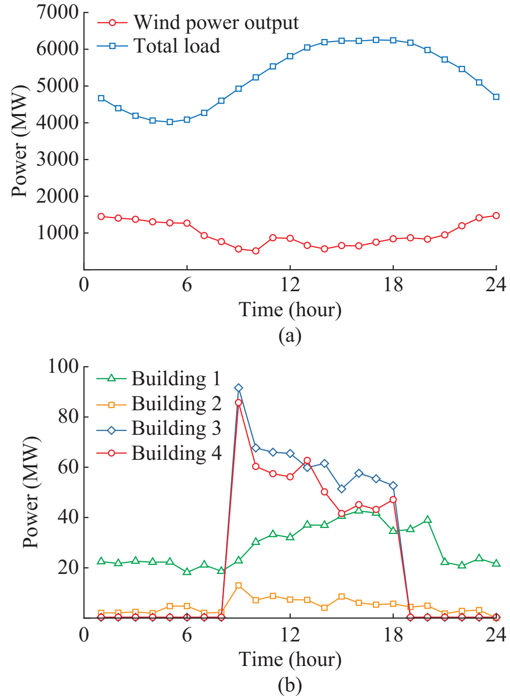

Fig. 7. Total load, wind power output, and AC power of four public public buildings. (a) Total load and wind power output. (b) AC power of four public public buildings.

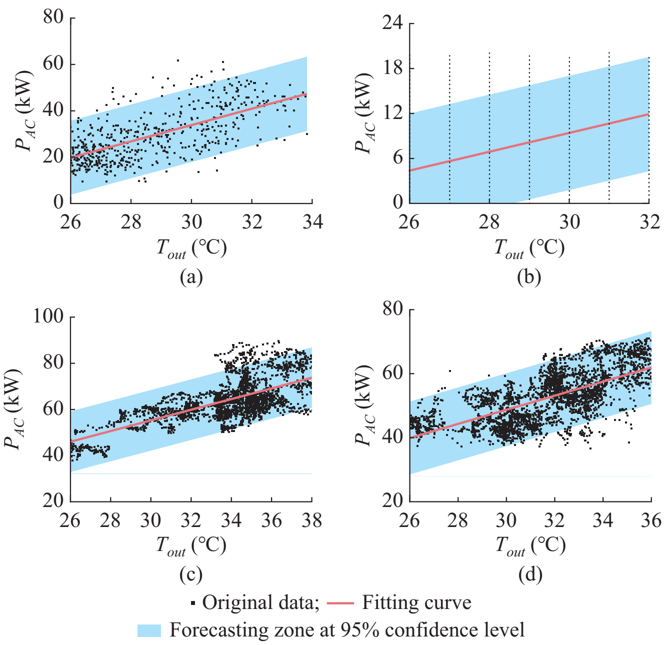

Fig. 8. Fitting results of four public buildings at 95% confidence level. (a) Building 1. (b) Building 2. (c) Building 3. (d) Building 4.

Generally, the effectiveness of linear fitting is described with the R-squared (R^2). In this paper, the R^2 values for the four public buildings are 0.46623, 0.35281, 0.48476, and 0.48509, respectively. For the real sample data, the fitting effect is regarded as good when the R^2 value is greater than 0.4. Therefore, the proposed evaluation method shows a good fitting performance for both CAC and VRV systems.

Among the four public buildings, building 1 has the largest fitting slope α, while building 2 has the smallest α. It means that the AC system in building 1 is more sensitive to outdoor temperature, showing a stronger DR potential. Conversely, the AC system in building 2 is less sensitive to outdoor temperature, resulting in a weaker DR potential. On the one hand, the AC system in building 2 has a smaller installed capacity, so the adjustable capacity is lower. On the other hand, the thermal inertia of the public building has a greater impact on the fitting slope α. As shown in (6)-(8), the greater the thermal resistance of the public building, the smaller the slope. Building 1 has a smaller thermal inertia, resulting in lower thermal resistance and a weaker building envelope. Therefore, more AC power is needed to maintain indoor temperature, leading to greater DR potential. Building 2 has a larger thermal inertia and stronger building envelope. Consequently, less AC power is needed to maintain the indoor temperature, resulting in a smaller adjustable capacity.

TABLE II
FITTING PARAMETERS OF FOUR PUBLIC BUILDINGS AT 95% CONFIDENCE LEVEL

Building	α	$\underline{\alpha}$	σ_α
Building 1	3.5211	3.2167	0.1550
Building 2	1.2556	1.2411	0.0074
Building 3	2.3084	2.2232	0.0435
Building 4	2.2029	2.1279	0.0382

The outdoor temperature sensor of building 2 has a measurement accuracy of only 1 ℃. As a result, the recorded outdoor temperature data only include integer values, making it appear discontinuous in Fig. 8. In contrast, the outdoor temperature sensors of buildings 1, 3, and 4 have a measurement accuracy of 0.1 ℃, which makes the data appear continuous in Fig. 8.

The fitting curves at different confidence levels of buildings 1 and 3 are shown in Figs. 9 and 10, respectively. As the confidence level increases, the bound of the fitting curve expands, encompassing more points within the interval. Conversely, when the confidence interval is smaller, the bound of the curve shrinks, resulting in fewer points falling within that interval. The downward bounds of α for buildings 1-4 are given in Table III. As the confidence level increases, the downward bound decreases, so the prediction interval will contain more points. The difference of $\underline{\alpha}$ between the 99% and the 50% confidence level for building 1 is 9.48%, and for building 3 is 3.77%. This indicates that there are much differences in bounds at different confidence levels, which can introduce bias into potential evaluation results. Therefore, these biases should be considered in practical potential evaluations utilizing the proposed evaluation method.

At the high confidence level interval, almost all points of building 1 are enveloped, while building 3 still has some points that are not enveloped. This is because building 1 uses a VRV system with simple control methods and fewer factors affecting power consumption. Building 3 uses a CAC system with complex control logic and more factors affecting AC power, such as outdoor temperature, outlet set temperature, and water pump operation frequency.

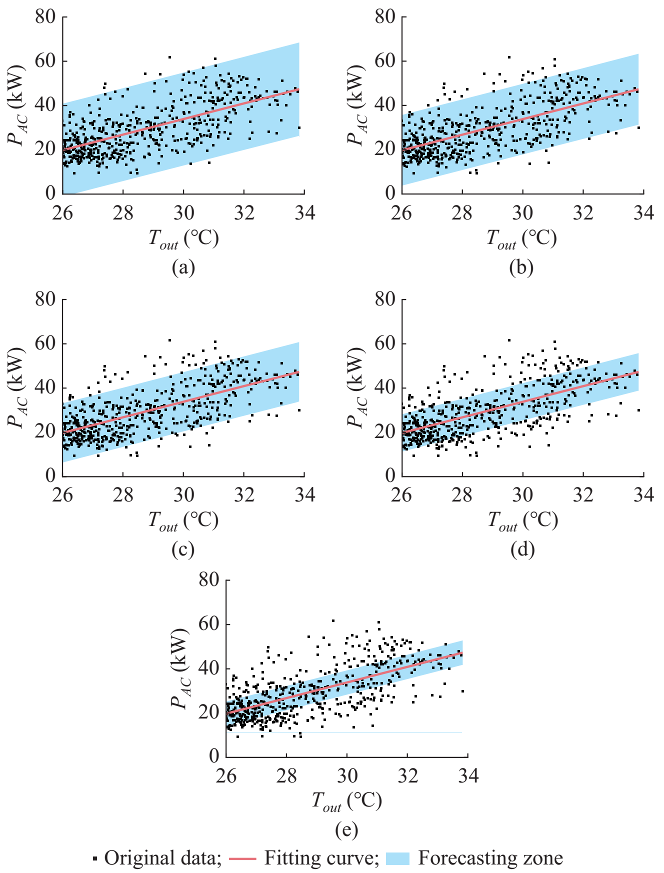

Fig. 9. Fitting curves of building 1 at different confidence levels. (a) $CL=99\%$. (b) $CL=95\%$. (c) $CL=90\%$. (d) $CL=70\%$. (e) $CL=50\%$.

The proposed evaluation method only considers the impact of outdoor temperature on AC power, which applies to both types of AC systems but has a better performance in VRV systems.

C. Evaluation Results

The temperature setting of buildings 1, 3, and 4 is increased by 3 °C. Building 2, which has a lower AC power and a higher temperature setting, will be increased by 1 °C. The baseline load curves for the four public buildings are respectively obtained from July 6, 2023, June 4, 2024, July 3, 2023, and July 4, 2023. Figure 11 shows the DR potential results for the four public buildings, where P_{base} is the baseline load of four public buildings. The higher the confidence level, the smaller the potential provided by the public building. For building 1, the mean relative error between 50% and 99% confidence levels is 9.48%. Compared with the 99% confidence level, the DR potential at the 10% confidence level is 12.21% larger. This is because the increased confidence level guarantees that the consumers are able to provide at least the regulation capacity. On the contrary, the lower the confidence level, the larger the potential. Without guaranteeing the confidence level, the consumers can provide more regulation potential. As the temperature setting undergoes further adjustments, the discrepancies observed at various confidence levels will widen, thereby introducing additional uncertainties and risks for LAs and ISOs.

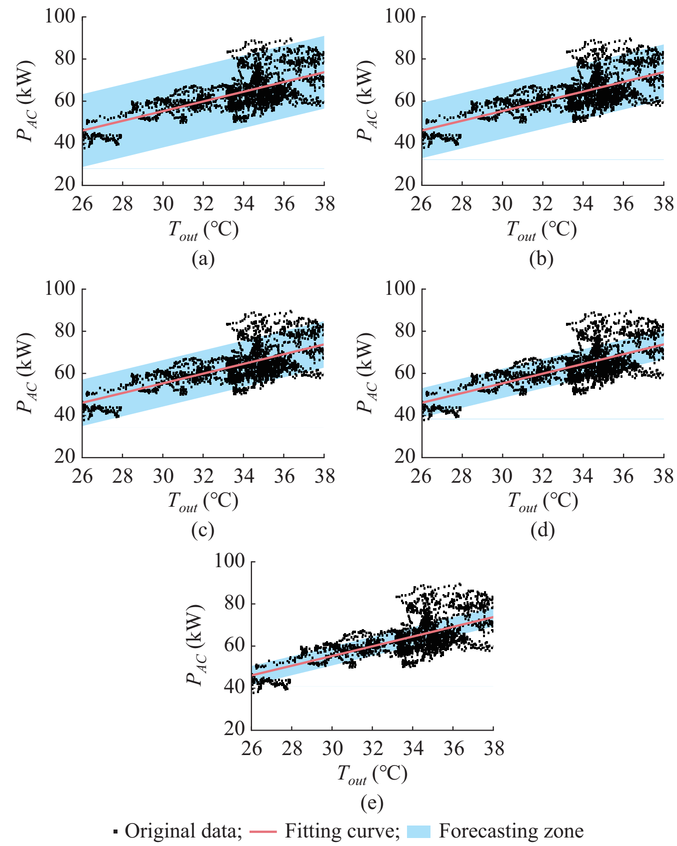

Fig. 10. Fitting curves of building 3 at different confidence levels. (a) $CL=99\%$. (b) $CL=95\%$. (c) $CL=90\%$. (d) $CL=70\%$. (e) $CL=50\%$.

TABLE III
DOWNWARD BOUNDS OF α AT DIFFERENT CONFIDENCE LEVELS

Building	Downward bound of α at different confidence levels				
	$CL=99\%$	$CL=95\%$	$CL=90\%$	$CL=70\%$	$CL=50\%$
Building 1	3.1206	3.2167	3.2658	3.3603	3.4165
Building 2	1.2365	1.2411	1.2434	1.2479	1.2506
Building 3	2.1964	2.2232	2.2369	2.2634	2.2791
Building 4	2.1043	2.1279	2.1399	2.1632	2.1771

The potential at the 99% confidence level differs the most from the deterministic evaluation results. For building 1, the deterministic evaluation result differs by 12.83% at the 99% confidence level. The deterministic evaluation does not consider the uncertainty of parameters, leading to an overestimation of the DR potential. For building 3 with a larger installed AC capacity, the deterministic evaluation result differs by 60.31% from the result at the 99% confidence level. For different public buildings, the larger the capacity, the greater the adjustable capacity, resulting in a larger difference between interval and deterministic evaluation results. The proposed evaluation method plays a more significant role in the evaluation of large-capacity AC systems. On the other hand, the potential evaluation result at the 10% confidence level is the closest to the deterministic evaluation results, indicating that the occurring probability of the deterministic evaluation results is very low, which may pose risks to system dispatch.

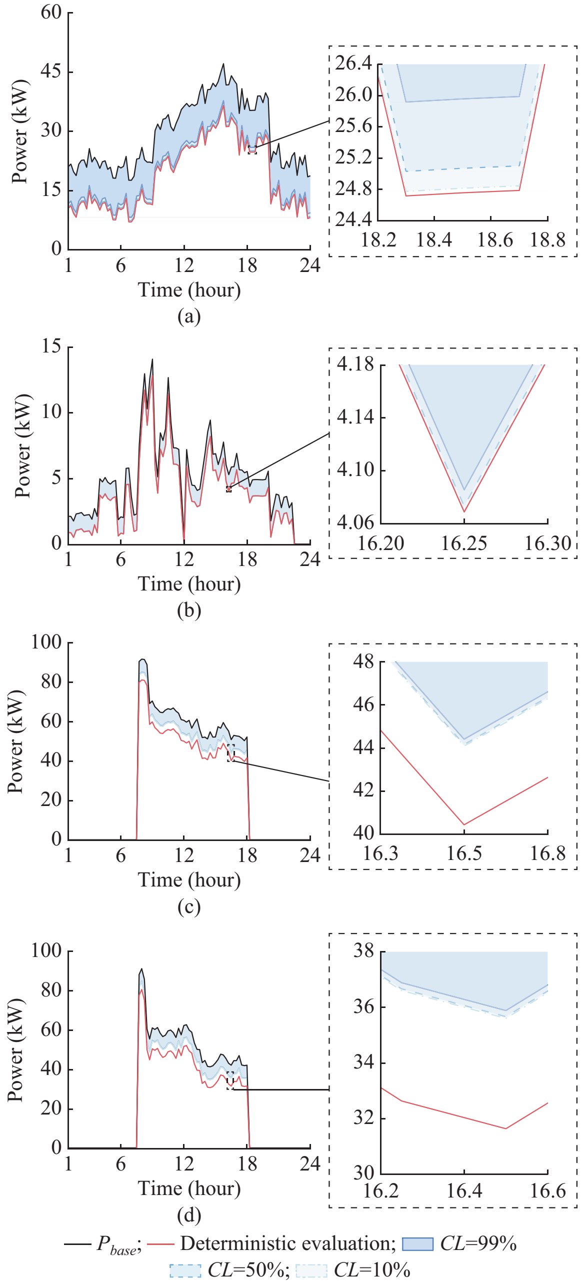

Fig. 11. DR potential results for four public buildings. (a) Building 1. (b) Building 2. (c) Building 3. (d) Building 4.

The evaluation results for the aggregation of the four public buildings are shown in Fig. 12. It can be observed that the gap between the deterministic evaluation and the probabilistic evaluation is larger after aggregation. It is especially evident during the daytime when AC power is higher. For instance, at 16:50, the deterministic evaluation differs from the probabilistic evaluation by 9.44 kW and 40.19%. For aggregated ACs, the aggregated capacity is relatively large, hence the proposed evaluation method becomes even more important. Assessment errors are further amplified after aggregation. Therefore, it is crucial to fully consider parameter uncertainties in the evaluation process. The proposed evaluation method ensures credible evaluation results under uncertainties, avoiding more risks compared with the deterministic evaluation and providing LAs or ISOs with variable evaluation results at different confidence levels.

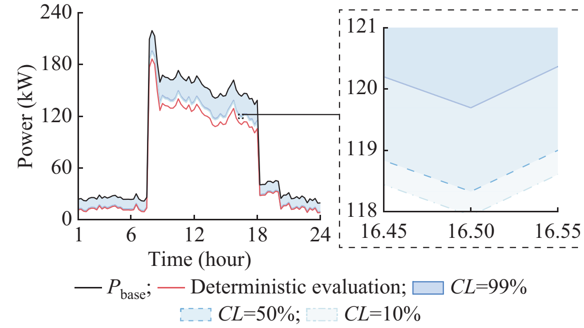

Fig. 12. Evaluation results for aggregation of four public buildings.

D. Risk Dispatch Result

The baseline loads of the four public buildings are scaled up by 10000 times. The proposed risk dispatch model is utilized to develop the generation plans for the thermal generators, while also allocating reserves to both the thermal generators and the public buildings. To validate the effectiveness of the proposed risk dispatch model, three simulation scenarios are set as follows.

1) Scenario 1: deterministic dispatch utilizing the deterministic potential evaluation results.

2) Scenario 2: dispatch considering the worst case, whose probability of the evaluated potential is smaller than $3\sigma_{\alpha}$.

3) Scenario 3: risk dispatch utilizing the proposed evaluation method, whose confidence level is set to be 99%.

Figure 13 illustrates the reserve allocation results of eight public buildings and Fig. 14 shows the online capacity of thermal generators. The reserve costs of public buildings for the three scenarios are \$7925844, \$8748674, and \$8218700, respectively. The public building reserves are allocated during 12:00-21:00, with no public building reserves arranged for the remaining periods. On the one hand, AC systems in public building are turned off at night, resulting in a very small adjustable capacity as shown in Fig. 11. Consequently, the public building reserve is minimal. On the other hand, the other periods do not coincide with peak load periods of the grid, leading to a minimal demand for public building reserves. Thus, there is no need for more expensive public buildings to provide public building reserves.

Compared with the deterministic dispatch in Scenario 1, both Scenario 2 and Scenario 3 arrange for more public building reserves to handle the uncertainty of public building reserve. At 17:00, the public building reserve in Scenario 2 is 8.56% higher than that in Scenario 1.

The public building reserve in Scenario 3 is 2.83% higher than that in Scenario 1. For building cluster 1, the public building reserve in Scenario 2 at 17:00 increases by 72.13% compared with that in Scenario 1, and the public building reserve in Scenario 3 decreases by 28.57% compared with that in Scenario 2. Although increasing public building reserve can enhance system reliability, it produces higher dispatch costs. The reserve cost in Scenario 2 is 10.38% higher than that in Scenario 1. While in Scenario 3, it is 3.69% higher than that in Scenario 1. Therefore, considering uncertainties in dispatch increases the public building reserves to cope with potential risks, which also raises dispatch costs. The public building reserve arranged in Scenario 3 is 5.57% less than that in Scenario 2, and the reserve cost in Scenario 2 is 6.45% higher. It indicates that Scenario 3 accepts a certain level of risk to reduce dispatch costs. The proposed risk dispatch model can balance risk and economy. In Fig. 14, Scenarios 1 and 2 have the same online capacity, but Scenario 3 has a smaller online capacity during 1:00-8:00. In risk dispatch, one thermal generator is shut down, so that the dispatch costs decrease.

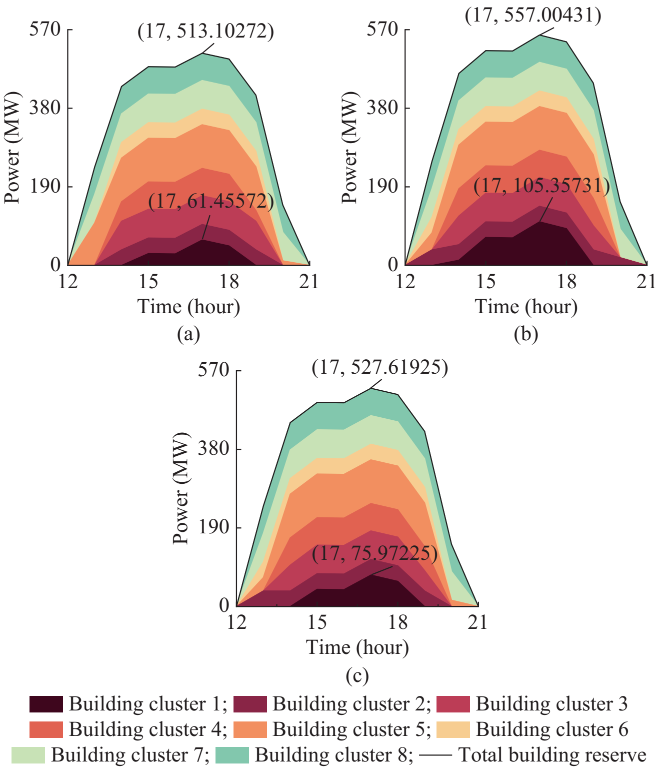

Fig. 13. Reserve allocation results of eight building clusters. (a) Scenario 1. (b) Scenario 2. (c) Scenario 3.

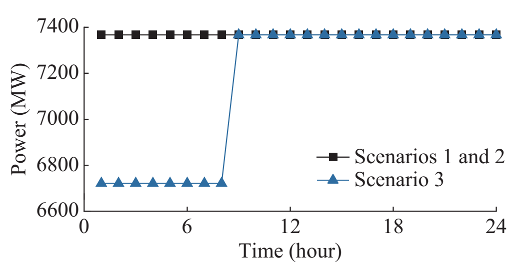

Fig. 14. Online capacity of thermal generators.

E. Dispatch Results at Different Confidence Levels and Uncertainties

The values of σ_α for building clusters 1-8 are set to be 0.2, 0.3, 0.4, 0.5, 0.2, 0.3, 0.4, and 0.5, respectively. The public building reserves are allocated at 55%, 75%, and 95% confidence levels, with the results shown in Fig. 15. It can be observed that for each building cluster, the higher the confidence level, the more reserves allocated. For building cluster 1, when the confidence level increases from 55% to 75%, the reserve increases by 12.55%. The reserve increases by 28.37% when the confidence level increases from 75% to 95%. It indicates that the closer the confidence level is to 1, the tighter the chance constraint, and the more reserves are required by the power system. The larger σ_α, the less capacity dispatched. For building clusters 1 and 5, which have the smallest uncertainty coefficients, the allocated capacity is the most. Conversely, for building clusters 4 and 8, which have the largest σ_α, the dispatched capacity is the least. Apparently, ISOs prefer public buildings with less uncertainty to ensure the security of the power system.

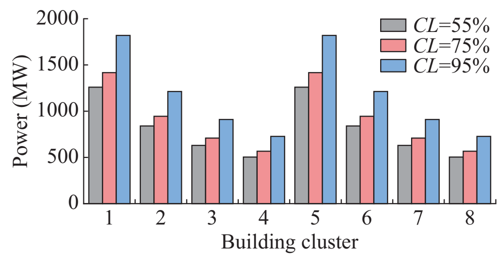

Fig. 15. Allocated reserve of eight building clusters at different confidence levels.

The cost coefficients for all eight building clusters are set to be 3500 $/MW. The uncertainty coefficients for the public buildings are all set to the same value, varying from 0.1 to 0.5. The confidence level varies from 55% to 95%, with a step size of 0.05. The reserve costs of public building clusters are shown in Fig. 16. The increases in the uncertainty coefficient and the confidence level result in higher dispatch costs. When the uncertainty coefficient is 0.1, sacrificing 5% of the confidence level (from 95% to 90%) reduces the cost by about 5%. When the uncertainty coefficient is 0.5, sacrificing 5% of the confidence level (from 95% to 90%) reduces the cost by about 15%. This indicates that public buildings with smaller uncertainty can significantly reduce dispatch costs. Under the same uncertainty coefficient of 0.5, increasing the confidence level from 50% to 55% raises the cost by 3.24%. However, increasing the confidence level from 90% to 95% raises the cost by 15.43%. The closer the confidence level is to 1, the more the gradient of cost increases, reaching a marginal effect. Therefore, it is important to choose an appropriate confidence level in real dispatch.

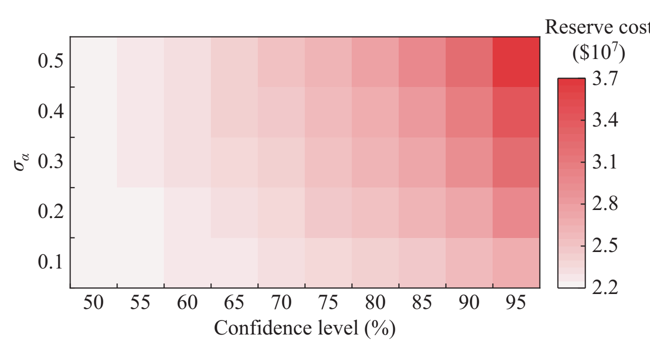

Fig. 16. Reserve costs at different confidence levels and uncertainties.

VI. CONCLUSION

The paper proposes the interval DR potential evaluation method and risk dispatch model to incorporate uncertain public buildings into power system operation. The proposed evaluation method quantifies the uncertainties of public buildings in practice and gives the credible interval DR potential. Furthermore, the risk dispatch model realizes a tradeoff between security and economy in power system operation. Numerical results illustrate that the error between deterministic evaluation and the proposed evaluation method with a 99% confidence level reaches 60.31%. The deterministic evaluation approximates the interval evaluation results with a 10% confidence level. Therefore, compared with deterministic evaluation, the proposed evaluation method performs better for public buildings with uncertainties. Moreover, the proposed evaluation plays a more significant role in large-capacity AC systems, especially for aggregated building clusters. Compared with the traditional deterministic dispatch model, the allocated reserves by the risk dispatch model are 2.83% more, which deals with the uncertainties of public buildings. Compared with the dispatch model considering the worst scenario, the reserve costs are 6.45% lower by the proposed risk dispatch model, which achieves better cost-effectiveness. Sacrificing a 5% confidence level, the costs will decrease by 15.43%. Following the proposed evaluation method in this paper, a bidding strategy for public buildings with uncertainties can be further studied in future research.

REFERENCES

[1] A. S. Malik and M. A. A. Umairi, "Cumulative capacity credit estimation for renewable energy projects," *Journal of Modern Power Systems and Clean Energy*, vol. 12, no. 5, pp. 1643-1651, Sept. 2024.

[2] T. Qi, C. Ye, and H. Hui, "Fast frequency regulation utilizing non-aggregate thermostatically controlled loads based on edge intelligent terminals," *IEEE Transactions on Smart Grid*, vol. 15, no. 4, pp. 3571-3584, Jul. 2024.

[3] H. Hui, Y. Ding, and M. Zheng, "Equivalent modeling of inverter air conditioners for providing frequency regulation service," *IEEE Transactions on Industrial Electronics*, vol. 66, no. 2, pp. 1413-1423, Feb. 2019.

[4] H. Zhong, J. Wang, H. Jia *et al*., "Vector field-based support vector regression for building energy consumption prediction," *Applied Energy*, vol. 242, pp. 403-414, May 2019.

[5] T. Qi, H. Hui, Y. Song *et al*., "Chance constrained economic dispatch of central air conditionings in large-scale commercial buildings considering demand response," *Energy and Buildings*, vol. 320, p. 114607, Oct. 2024.

[6] P. Domingues, P. Carreira, R. Vieira *et al*., "Building automation systems: concepts and technology review," *Computer Standards & Interfaces*, vol. 45, pp. 1-12, Mar. 2016.

[7] A. Rodler, S. Guernouti, M. Musy *et al*., "Thermal behaviour of a building in its environment: modelling, experimentation, and comparison," *Energy and Buildings*, vol. 168, pp. 19-34, Jun. 2018.

[8] A. Ghahramani, C. Tang, and B. Becerik-Gerber, "An online learning approach for quantifying personalized thermal comfort via adaptive stochastic modeling," *Building and Environment*, vol. 92, pp. 86-96, Oct. 2015.

[9] N. Lu, "An evaluation of the HVAC load potential for providing load balancing service," *IEEE Transactions on Smart Grid*, vol. 3, no. 3, pp. 1263-1270, Sept. 2012.

[10] W. Li, L. Yang, and Y. Ji, "Estimating demand response potential under coupled thermal inertia of building and air-conditioning system," *Energy and Buildings*, vol. 182, pp. 19-29, Jan. 2019.

[11] Y. Chen, P. Xu, H. Wang *et al*., "Experimental investigation of demand response potential of buildings: combined passive thermal mass and active storage," *Applied Energy*, vol. 280, p. 115956, Dec. 2020.

[12] C. Gehbauer, E. S. Lee, and T. Wang, "An evaluation of the demand response potential of integrated dynamic window and HVAC systems," *Energy and Buildings*, vol. 298, p. 113481, Nov. 2023.

[13] Z. Wang, P. Yu, and H. Zhang, "Privacy-preserving regulation capacity evaluation for HVAC systems in heterogeneous buildings based on federated learning and transfer learning," *IEEE Transactions on Smart Grid*, vol. 14, no. 5, pp. 3535-3549, Sept. 2023.

[14] M. Afzalan and F. Jazizadeh, "Residential loads flexibility potential for demand response using energy consumption patterns and user segments," *Applied Energy*, vol. 254, p. 113693, Nov. 2019.

[15] J. Zhu, J. Niu, and Z. Tian, "Rapid quantification of demand response potential of building HAVC system via data-driven model," *Applied Energy*, vol. 325, p. 119796, Nov. 2022.

[16] H. Long, C. Zhang, R. Geng *et al*., "A combination interval prediction model based on biased convex cost function and auto-encoder in solar power prediction," *IEEE Transactions on Sustainable Energy*, vol. 12, no. 3, pp. 1561-1570, Jul. 2021.

[17] Y. Sun, Y. Zhou, S. Wang *et al*., "Nonparametric probabilistic prediction of regional PV outputs based on granule-based clustering and direct optimization programming," *Journal of Modern Power Systems and Clean Energy*, vol. 11, no. 5, pp. 1450-1461, Sept. 2023.

[18] C. Zhang and Y. Fu, "Probabilistic electricity price forecast with optimal prediction interval," *IEEE Transactions on Power Systems*, vol. 39, no. 1, pp. 442-452, Jan. 2024.

[19] M. Song, W. Sun, Y. Wang *et al*., "Hierarchical scheduling of aggregated TCL flexibility for transactive energy in power systems," *IEEE Transactions on Smart Grid*, vol. 11, no. 3, pp. 2452-2463, May 2020.

[20] S. Faddel, Q. Sun, and G. Tian, "Modeling and coordination of commercial buildings in distribution systems," *IEEE Transactions on Industry Applications*, vol. 58, no. 2, pp. 1654-1663, Mar. 2022.

[21] Z. Rostamnezhad, N. Mary, and L. A. Dessaint, "Electricity consumption optimization using thermal and battery energy storage systems in buildings," *IEEE Transactions on Smart Grid*, vol. 14, no. 1, pp. 251-265, Jan. 2023.

[22] Y.-E. Jang, Y.-J. Kim, and J. P. S. Catalão, "Optimal HVAC system operation using online learning of interconnected neural networks," *IEEE Transactions on Smart Grid*, vol. 12, no. 4, pp. 3030-3042, Jul. 2021.

[23] Z. Li, S. Su, X. Jin *et al*., "Stochastic and distributed optimal energy management of active distribution networks within integrated office buildings," *CSEE Journal of Power and Energy Systems*, vol. 10, no. 2, pp. 504-517, Mar. 2024.

[24] Z. Song, J. Shi, S. Li *et al*., "Data-driven and physical model-based evaluation method for the achievable demand response potential of residential consumers' air conditioning loads," *Applied Energy*, vol. 307, p. 118017, Feb. 2022.

[25] A. P. A. da Silva and L. S. Moulin, "Confidence intervals for neural network based short-term load forecasting," *IEEE Transactions on Power Systems*, vol. 15, no. 4, pp. 1191-1196, Nov. 2000.

[26] P. G. Hoel, "Confidence regions for linear regression," in *Proceedings of the Second Berkeley Symposium on Mathematical Statistics and Probability*, Berkeley, USA, Feb. 1951, pp. 75-82.

[27] J. Pfanzagl and O. Sheynin, "A forerunner of the *t*-distribution (studies in the history of probability and statistics XLIV)," *Biometrika*, vol. 83, no. 4, pp. 891-898, Mar. 1996.

[28] P. Li, H. Arellano-Garcia, and G. Wozny, "Chance constrained programming approach to process optimization under uncertainty," *Computers & Chemical Engineering*, vol. 32, no. 1, pp. 25-45, Jan. 2008.

[29] X. Geng and L. Xie, "Data-driven decision making in power systems with probabilistic guarantees: theory and applications of chance-constrained optimization," *Annual Reviews in Control*, vol. 47, pp. 341-363, Jan. 2019.

[30] J. Li, H. Zeng, and Y. Xie, "Unit commitment with joint chance constraints in multi-area power systems with wind power based on partial sample average approximation," *Journal of Modern Power Systems and Clean Energy*, vol. 13, no. 1, pp. 241-252, Jan. 2025.

[31] X. Zhao, Q. Xu, and Y. Yang, "Service restoration of distribution system considering novel battery charging and swapping station, repair crews, and network reconfigurations," *Journal of Modern Power Systems and Clean Energy*, vol. 12, no. 6, pp. 1905-1917, Nov. 2024.

[32] S. Kang, M. Lee, and R. A. de Callafon, "Q-convergence with interquartile ranges," *Journal of Economic Dynamics and Control*, vol. 29, no. 10, pp. 1785-1806, Oct. 2005.

[33] P. Sun, L. Huo, and X. Chen, "Rotor angle stability prediction using temporal and topological embedding deep neural network based on grid-informed adjacency matrix," *Journal of Modern Power Systems and Clean Energy*, vol. 12, no. 3, pp. 695-706, May 2024.

[34] South China Energy Regulatory Bureau of National Energy Adminis-

tration of the People's Republic of China. (2022, Jun.). Implementation guidelines for power auxiliary service management in the southern region. [Online]. Available: https://nfj.nea.gov.cn/file_upload/20220613/3921655118300332_9693ce64-2d9e-422d-a0d9-3b017a3556b5.pdf

[35] Guangdong Power Exchange Center. (2022, Apr.). Implementation guidelines for market-based demand response in Guangdong Province. [Online]. Available: https://guangdongsd.chnenergy.com.cn/dlyxww/zcfga/202303/ef890f0072234f24a3144329a34f8e97/files/aa4a553aa4c54c7f849c4aaf854ba491.pdf

Yu Yao received the B.S. degree in electrical engineering from North China Electric Power University, Baoding, China, in 2020. He is currently pursuing the Ph.D. degree with the College of Electrical Engineering, Zhejiang University, Hangzhou, China. His research interests include demand response, public building, and power system optimization.

Chengjin Ye received the B.E. and Ph.D. degrees in electrical engineering from Zhejiang University, Hangzhou, China, in 2010 and 2015, respectively. From 2015 to 2017, he served as a Distribution System Engineer with the Economics Institute, State Grid Zhejiang Electric Power Company Ltd., Hangzhou, China. From 2017 to 2019, he was an Assistant Research Fellow with the College of Electrical Engineering, Zhejiang University. Since 2020, he has been a Tenure-track Professor. His research interests include resilience enhancement of power grid and integrated energy system, as well as market mechanism and control strategy towards integration of demand resource into power system optimization.

Yuming Zhao received the B.S. and Ph.D. degrees from the Department of Electrical Engineering, Tsinghua University, Beijing, China, in 2001 and 2006, respectively. He is currently a Senior Engineer (Professor level) with Shenzhen Power Supply Co., Ltd., Shenzhen, China. His research interest includes DC distribution network.

Yi Ding received the B.S. degree in electrical engineering from Shanghai Jiao Tong University, Shanghai, China, in 2002, and the Ph.D. degree in electrical engineering from Nanyang Technological University, Singapore, in 2007. He is currently a Professor at the College of Electrical Engineering, Zhejiang University, Hangzhou, China. His current research interests include power system reliability analysis incorporating renewable energy resource, smart grid performance analysis, and engineering system reliability modeling and optimization.